RECONSTRUCTING EXCAVATION CAVITY SHAPES FROM ANOMALOUS RIM HEIGHT VARIATIONS IN FRESH LUNAR CRATERS. V. L. Sharpton[1], E. Lalor[1] and P. J. Mouginis-Mark[2], [1]Lunar and Planetary Institute (3600 Bay Area Blvd., Houston, TX 77058; sharpton@lpi.usra.edu), [2]Hawaii Institute Geophysics Planetology, University of Hawaii, Honolulu, Hawaii 96822 (pmm@higp.hawaii.edu).

Introduction: For near-vertical trajectories, the initial product of crater excavation is believed to be a circular, bowl-shaped cavity that is subsequently modified by gravity driven collapse [1]. This implies that deviations from circularity in the final crater rim (e.g., Fig. 1) are generated solely during late-stage modification. If so, final rim height (h) should be a simple function of range (r) from the crater center. Here we use a set of 26 fresh lunar craters (10 km ≤ D ≤ 50 km) to test this hypothesis. Results show that, for many craters produced by near-vertical impacts, a significant portion of rim topography is not consistent with late-stage collapse of a radially symmetric excavation cavity. Such anomalous rim properties appear to indicate asymmetries in the excavation cavity induced by target strength variations and/or the effects of non-vertical impact trajectories. Finally, we reconstruct an excavation cavity shape that is consistent with measured rim heights.

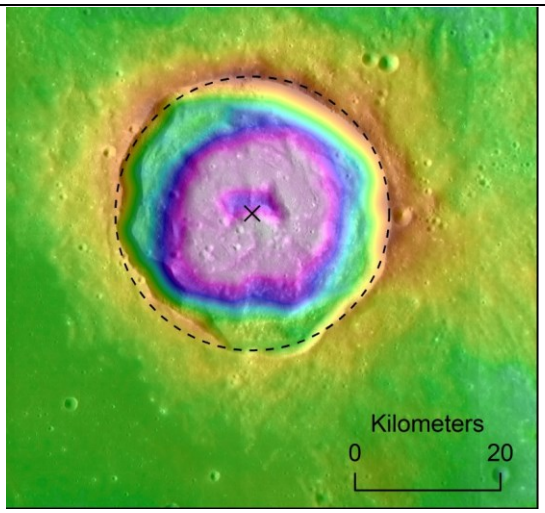

Fig. 1: *38-km Manilius crater showing varitions in rim crest. Circle of average rim radius is shown by dashed line; × shows the centroid of the rim crest shape. Rim heights reveal significant asymmetries unaccounted for with a radially symmetric excavation cavity.*

Method: Apparent DEMs (i.e., with elevations referenced to the pre-impact surface) were produced for each crater using the approach of [2]. The rim crest profile of each crater then encloses a polygon whose centroid constrains the crater center and from which the average crater radius (R) and average rim height (H) are calculated. R and H define the properties of a radially symmetric 'reference crater'. We assume that the reference crater abides by the model presented by [3], with appropriate modifications, see [2]:

$h/H=C(r/R)^B$ where $B = -3$ [equation 1].

Setting C=1 and using local r(θ) and h(θ), where θ denotes bearing from center, yields the amount of local rim height (Δh(θ)) that is inconsistent with collapse of a radially symmetric excavation cavity (e.g., Fig. 2).

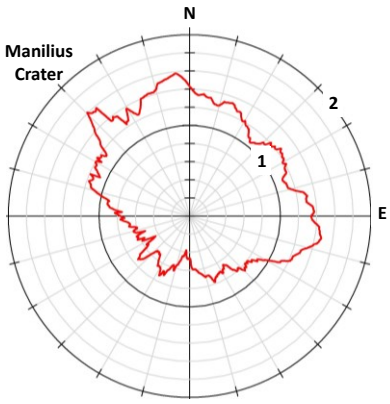

Fig. 2: *Polar plot of anomalous rim height Δh(θ) (red line) shown as fraction of h/H=1 (inner black circle, the reference crater). Where h/H >1, rim is higher than predicted by the radially symmetric model. Likewise, rim heights are deficient where h/H <1.*

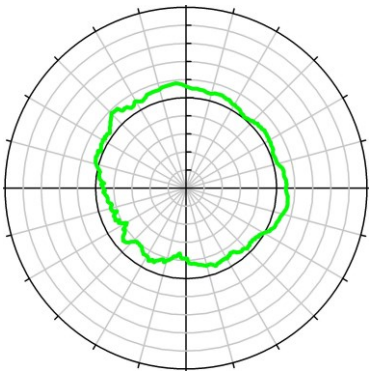

Fig. 3: *Reconstructed shape of Manilius' excavation cavity (green line) that is consistent with both radius and elevation characteristics of its rim crest. Inner black circle shows average radius of excavation cavity, R_{ex}. Gray lines show deviation increments of 0.2 R_{ex}.*

To derive the shape of an excavation cavity that is consistent with each crater's rim properties, we invert equation 1 at each point on the rim profile to solve for a local dimensionless range (i.e., $r(\theta)/R_{ex}=1$) that is consistent with the measured h/H (e.g., Fig. 3).

Results and discussion: All craters studied showed significant amounts of rim topography that is unaccounted for in the radially symmetric excavation cavity model (Fig. 4). This anomalous rim topography provides useful insights into the local and regional properties that influence crater excavation.

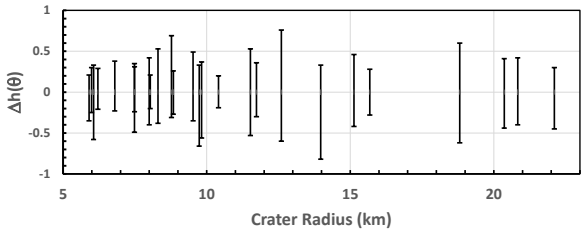

Fig. 4: *Range of Δh(θ) as a fraction of h(θ) for each of the 26 craters studied. A circular excavation cavity would show as a point at Δh(θ)=0.*

In general, two end-member forms emerge in the polar Δh(θ) plots (Figs 2 and 5b):

- ***Offset patterns***, where the center of the Δh(θ) pattern is displaced from the center of the reference circle. These patterns point to zonal differences in target properties that influence the effectiveness of excavation in one or more sectors of the crater. This is illustrated by Manilius (Fig. 2), where Δh(θ) shows significant positive excursions between N60W and S60E (i.e., bearings between θ = 300° and 120°), wherein Δh(θ) shows positive excursions approaching 50% of h(θ). This pattern is coupled with a complementary section of rim crest toward the S and SW that is anomalously low. Such patterns appear consistent with the effects produced by local differences in excavation efficiency. For instance, the elongation in Manilius' calculated zone of excavation (Fig. 3) between 300° and 120° suggests that target material was more effectively displaced in that sector of the crater.
- ***Bilaterally symmetric patterns*** (e.g., Kepler crater, Fig. 5), where the Δh(θ) pattern is elongated about the center in one direction (NE-SW in Fig. 5b) and reduced with respect to the reference crater in the orthogonal direction. These patterns signal an elongate excavation cavity such as might be produced by oblique impact events (e.g. [4]). Kepler's final crater rim and ejecta pattern are remarkably circular and it exhibits none of the other morphological signs of low-angle impact (e.g. [4,5]. Consequently, if its Δh(θ) characteristics are indicative of a non-vertical trajectory, it may be a more sensitive indicator of impact angle than those other morphological signs. On the other hand, it is possible that a strong regional stress field could influence excavation and generate an elongate cavity. This has been shown to be the case for Barringer Crater in Arizona [2,6,7]. Further work is required to determine which, if either, of these possibilities is responsible for Kepler's excavation cavity characteristics.

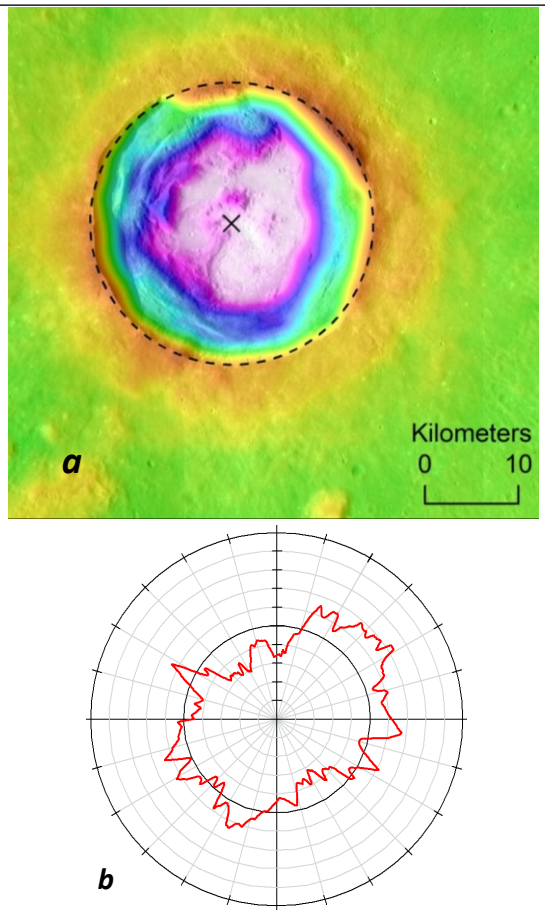

Fig. 5: ***a***. DEM of Kepler crater (R=15.1 km) showing variations in rim height and position compared to average radius (dashed line) and center (×). ***b***. Symmetrical Δh(θ) pattern of Kepler indicative of either the effects of oblique impact trajectory or the influence of a regional stress field.

References: [1] Melosh H. J. and Ivanov B. A. (1999) *Ann. Rev. Earth Planet. Sci. 27,* 385–415. [2] Sharpton V. L. (2014) *JGR 119,* 154–168, doi:10.1002/2013JE004523. [3] McGetchin T. R. et al. (1973) *EPSL 20,* 226–236. [4] Pierazzo E. and Melosh H. J. (2000) *Ann. Rev. Earth Planet. Sci. 28,* 141–167. [5] Schultz P. H. and Anderson R. R. (1996) *Geol. Soc. Am. Spec. Pap. 302*, 397-417. [6] Kumar P. S. and Kring D. A. (2007) *JGR 113*, E09009, doi:10.1029/2008JE003115. [7] Poelchau, M. H. et al. (2009) *JGR 114*, E01006, doi:10.1029/2008JE003235.